iScience

CellPress
OPEN ACCESS

Article

A novel mouse AAV6 hACE2 transduction model of wild-type SARS-CoV-2 infection studied using synDNA immunogens

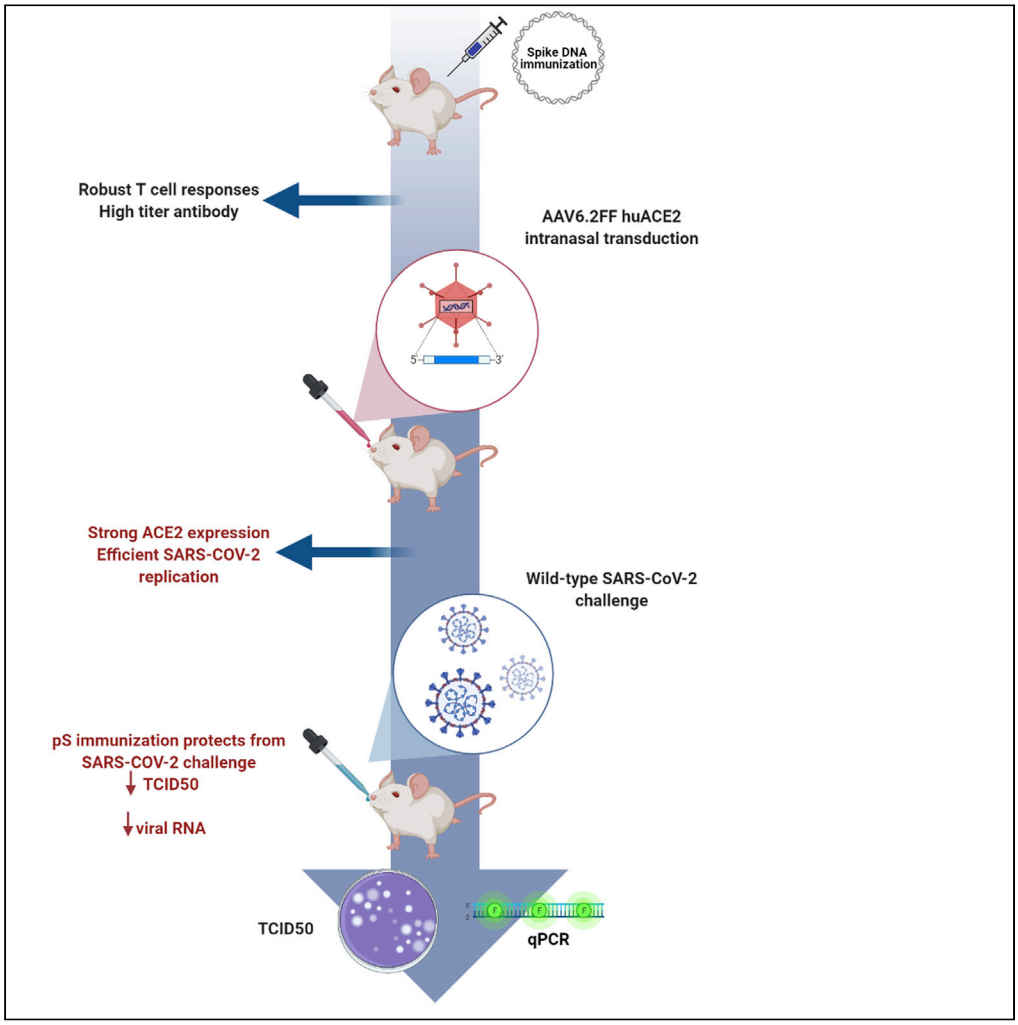

Ebony N. Gary, Bryce M. Warner, Elizabeth M. Parzych, ..., Ami Patel, David B. Weiner, Darwyn Kobasa

dweiner@wistar.org (D.B.W.)
darwyn.kobasa@canada.ca (D.K.)

Highlights

AAV6 transduction of human ACE2 supports wild-type SARS-CoV-2 infection in mice

A synDNA vaccine expressing SARS-CoV-2 spike is immunogenic in mice

Spike DNA immunization protects mice from SARS-CoV-2 challenge

Gary et al., iScience 24, 102699
July 23, 2021
https://doi.org/10.1016/j.isci.2021.102699

iScience

CellPress
OPEN ACCESS

Article

A novel mouse AAV6 hACE2 transduction model of wild-type SARS-CoV-2 infection studied using synDNA immunogens

Ebony N. Gary,[1,6] Bryce M. Warner,[2,6] Elizabeth M. Parzych,[1,6] Bryan D. Griffin,[2,6] Xizhou Zhu,[1,6] Nikesh Tailor,[2] Nicholas J. Tursi,[1] Mable Chan,[2] Mansi Purwar,[1] Robert Vendramelli,[2] Jihae Choi,[1] Kathy L. Frost,[2] Sophia Reeder,[1] Kevin Liaw,[1] Edgar Tello,[1] Ali R. Ali,[1] Kun Yun,[1] Yanlong Pei,[3] Sylvia P. Thomas,[3] Amira D. Rghei,[3] Matthew M. Guilleman,[3] Kar Muthumani,[1] Trevor Smith,[4] Sarah K. Wootton,[3] Ami Patel,[1] David B. Weiner,[1,7,*] and Darwyn Kobasa[2,5,*]

SUMMARY

More than 100 million people have been infected with severe acute respiratory syndrome coronavirus-2 (SARS-CoV-2). Common laboratory mice are not susceptible to wild-type SARS-CoV-2 infection, challenging the development and testing of effective interventions. Here, we describe the development and testing of a mouse model for SARS-CoV-2 infection based on transduction of the respiratory tract of laboratory mice with an adeno-associated virus vector (AAV6) expressing human ACE-2 (AAV6.2FF-hACE2). We validated this model using a previously described synthetic DNA vaccine plasmid, INO-4800 (pS). Intranasal instillation of AAV6.2FF-hACE2 resulted in robust hACE2 expression in the respiratory tract. pS induced robust cellular and humoral responses. Vaccinated animals were challenged with 10^5 $TCID_{50}$ SARS-CoV-2 (hCoV-19/Canada/ON-VIDO-01/2020) and euthanized four days post-challenge to assess viral load. One immunization resulted in 50% protection and two immunizations were completely protective. Overall, the AAV6.2FF-hACE2 mouse transduction model represents an easily accessible, genetically diverse mouse model for wild-type SARS-CoV-2 infection and preclinical evaluation of potential interventions.

INTRODUCTION

In December 2019 a novel coronavirus was identified as the etiological agent of a severe acute respiratory syndrome (**SARS**)-like disease in Wuhan China (Zhu et al., 2020; Zhou et al., 2020). The previously unknown betacoronavirus, now identified as severe-acute respiratory syndrome coronavirus-2 (SARS-CoV-2), causes coronavirus disease-2019 (**COVID-19**) and has spread rapidly from person to person causing a global pandemic. SARS-CoV-2 is the seventh coronavirus disease known to infect humans. It is similar to, but distinct from Middle East respiratory syndrome coronavirus (**MERS-CoV**) and severe acute respiratory syndrome coronavirus-1 (**SARS-CoV-1**), both of which have caused outbreaks this century. Like both MERS-CoV and SARS-CoV-1, SARS-CoV-2 is suspected to be of bat origin with an intermediate host. To date SARS-CoV-2 has infected more than 100 million people and caused over two million deaths worldwide. COVID-19 is characterized by fever, cough, and pneumonia (Huang et al., 2020); however, lower gastrointestinal symptoms such as diarrhea have been reported (Jin et al., 2020). The rapid person-to-person spread of SARS-CoV-2, the increasingly noted potential for asymptomatic spread, and the severe burden being placed on global health infrastructure, necessitated the rapid development of effective vaccines and therapeutics. Fortunately, three vaccines have been approved for emergency use in the United States to date, with many other candidates in clinical trials. The evaluation of these potential interventions requires the development of new tools for studying SARS-CoV-2 infection.

To date a lack of appropriate small animal models for SARS-CoV-2 virus infection has been a significant hurdle for preclinical evaluation of potential vaccine candidates and therapeutics. Like SARS-CoV-1, angiotensin converting enzyme-2 (**ACE2**) is the cellular receptor for SARS-CoV-2. However, mouse ACE2 does

[1]The Vaccine and Immunotherapy Center, The Wistar Institute, Philadelphia, PA, USA

[2]Public Health Agency of Canada, Winnipeg, MB, Canada

[3]Ontario Veterinary College, University of Guelph, Guelph, ON, Canada

[4]Inovio Pharmaceuticals, San Diego, CA, USA

[5]Department of Medical Microbiology, University of Manitoba, Winnipeg, MB, Canada

[6]These authors contributed equally

[7]Lead contact

*Correspondence: dweiner@wistar.org (D.B.W.), darwyn.kobasa@canada.ca (D.K.)

https://doi.org/10.1016/j.isci.2021.102699

not permit wild-type SARS-CoV-2 infection. In an effort to bypass this restriction, several models are being evaluated. These include a transgenic mouse model expressing human ACE2 (hACE2) (Yang et al., 2007; Moreau et al., 2020; Winkler et al., 2020). This model is an important new tool; however, it is currently restricted to the C57BL/6 mouse background. The Syrian hamster model has also been implemented for the study of SARS-CoV-2 infection. SARS-CoV-2 replicates efficiently in the hamster lung and causes pathological lesions which recapitulates human disease (Imai et al., 2020). However, due to the abundance of reagents, the cost-efficiency, and the ease of use, adapting diverse mouse strains for infection by wild-type SARS-CoV-2 strains would be an additional important tool for studying pathogenesis, therapeutics, and vaccines.

Adenovirus-transduced models are also under evaluation (Hassan et al., 2020; Zost et al., 2020). Additionally, adenoviruses are immune stimulatory in mice in mice which might limit some measured SARS-CoV-2 infection responses. We previously reported that a modified version of the immune "silent" adeno-associated virus-6 (**AAV6.2FF**) can engender robust transgene expression in the lungs of mice when delivered intranasally (van Lieshout et al., 2018). In order to model SARS-CoV-2 infection in diverse and easily accessible mouse models, we generated an AAV6.2FF vector expressing human ACE2 (**AAV6-2FF.hACE2**). We show that intranasal instillation of AAV6-2FF.hACE2 resulted in robust hACE2 expression in the lungs of mice and permitted successful replication of a clinical SARS-CoV-2 isolate.

We used the clinical candidate INO-4800, a DNA vaccine plasmid encoding the full-length spike (**S**) glycoprotein of SARS-CoV-2 (**pS**) to validate the AAV6-2FF.hACE2 transduction model. pS vaccination induced SARS-CoV-2 spike receptor binding domain (RBD)-binding IgG in the serum of immunized animals and significantly enhanced cellular responses. Anti-spike antibodies persisted more than 80 days and were capable of neutralizing SARS-CoV-2 spike-pseudotyped viruses *in vitro*. In the AAV6.2FF.hACE2 model, two pS immunizations completely controlled lung viral replication as compared to control animals. This strongly correlated with increased total antibody and neutralizing antibody titers in serum prior to challenge. These results support the utility of hACE2 transduction models for wild-type SARS-CoV-2 infection studies and indicate that this model will be useful for evaluation of preclinical COVID-19 interventions.

RESULTS

Characterizing an AAV6.2FF-hACE2 transduction model for SARS-CoV-2 infection of wild-type mice

Since murine ACE2 does not serve as a receptor for SARS-CoV-2 (Bao et al., 2020), and based on the initial limited availability, expense, and lack of strain diversity of hACE2 transgenic mice, we elected to engineer a highly lung tropic AAV vector, termed AAV6.2FF (Van Lieshout et al., 2018), to deliver the hACE2 gene (Figures 1A and 1B) to the lung of vaccinated mice to render them susceptible to challenge with SARS-CoV-2. Previous studies have demonstrated that AAV6.2FF can mediate long term (>200 days) transgene expression in the murine lung in both alveolar type 2 and club (Clara) cells (Kang et al., 2020; Santry et al., 2017; van Lieshout et al., 2018). When we delivered a control version of this vector expressing luciferase, we observed robust luminescence (Figure 1C) using a modified intranasal method of administration that ensures delivery of the vector to the entire respiratory tract, including the distal lung. To investigate whether mice transduced with AAV6.2FF-hACE2 were permissive for SARS-CoV-2 replication, mice transduced with 1 x 10^{11}viral genomes of the vector were challenged 10 days later with 1 × 10^5 PFU of SARS-CoV-2 VIDO-01 P2 delivered intranasally. Mice were euthanized on days 2 and 4 post-challenge and viral RNA copy number determined by qRT-PCR. Mice infected with AAV6.2FF-luc showed significant luciferase expression in the lungs beginning as early as day 3 and lasting through day 10 (Days 3, 5, 7 not shown). Day 10 shown in Figure 1C). Both male and female BALB/c mice given AAV expressing human ACE2 had high levels of SARS-CoV-2 in the upper and lower lungs on days 2 and 4 post-infection while those that received AAV expressing luciferase did not have detectable virus, consistent with previous findings that wild type mice are not susceptible to SARS-CoV-2 infection (Figures 1E and 1F). Comparable levels of viral RNA and live virus were seen in the nasal turbinate of both hACE2 and luciferase transduced mice suggesting that hACE2 expression is likely confined mostly to the lungs, consistent with our luciferase data and previous publications (van Lieshout et al., 2018) (Figures 1E and 1F). Overall, this model resulted in high levels of viral replication in the lungs of transduced and SARS-CoV-2 infected mice. This provided us with a suitable challenge model using a wild-type isolate of SARS-CoV-2.

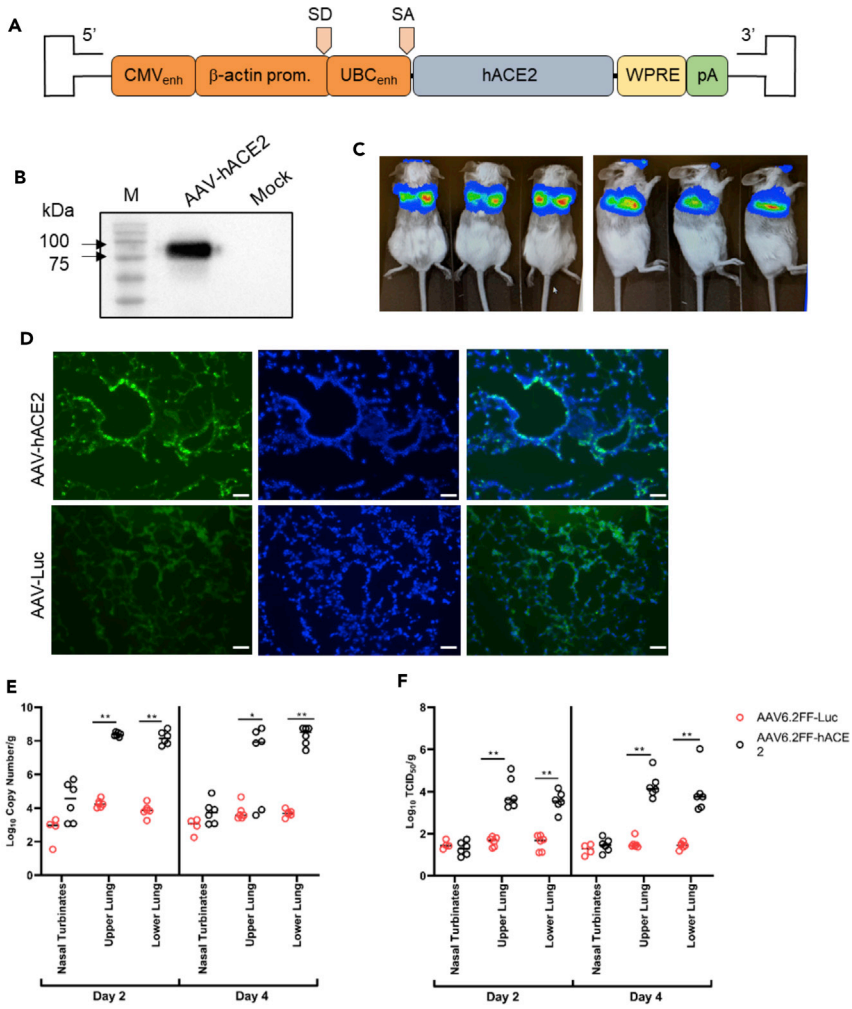

Figure 1. Characterization of an AAV6.2FF-hACE2 transduction model for SARS-CoV-2 infection of wild-type mice

(A) Diagram of AAV genome expressing hACE2 from the CASI promoter.

(B) Western blot of HEK293 cells transduced with AAV6.2FF-hACE and probed with an anti-hACE2 antibody.

(C) BALB/c mice were administered 1 x 10^{11}vg of AAV-Luc intranasally and imaged 10 days later using an IVIS imager.

(D–F) (D) IFA images of lungs harvested from BALB/c mice infected intranasally with 1 x 10^{11}vg of AAV-hACE2 or AAV-Luc and euthanized 10 days later. Lungs were stained with a rabbit anit-hACE2 antibody and imaged at 20 X (scale bar, 50mM). Viral RNA (E), and virus TCID50 titers (F) were determined in respiratory tissues on days 2 and 4 post-infection. n = 6 (3M, 3F). Statistical significance determined by Mann-Whitney test. * = $p < 0.05$, ** = $p < 0.01$.

pS immunization induces robust IFNγ T cell responses

We hypothesized that this model would allow us to evaluate preclinical efficacy of this DNA vaccine in a mouse model of SARS-CoV-2 infection. Mice were immunized twice, separated by 4 weeks, by intramuscular injection followed by *in vivo* electroporation (Figure 2A). Animals were euthanized at day 7 postimmunization and IFNγ-secreting cells in the spleen were enumerated by ELISpot after stimulation with overlapping spike peptides covering the entire spike protein from SARS-CoV-2, SARS-CoV-1, and MERS-CoV. Mice immunized with pS had increased IFNγ-secreting T cells in their spleens (Figures 2B, 2E, and 2H). We also observed IFNγ secretion in response to stimulation with SARS-CoV-1 peptides, likely due to the high sequence homology shared between SARS-CoV-2 and SARS-CoV-1 (Figures 2C, 2F, and 2I). We observed no IFNγ secretion in response to stimulation with MERS-CoV stimulation (Figures 2D, 2G, and 2J). These data indicate that pS immunization induces robust IFNγ-mediated cellular immunity and suggest that anti-SARS-CoV-1 and anti-SARS-CoV-2 responses may overlap.

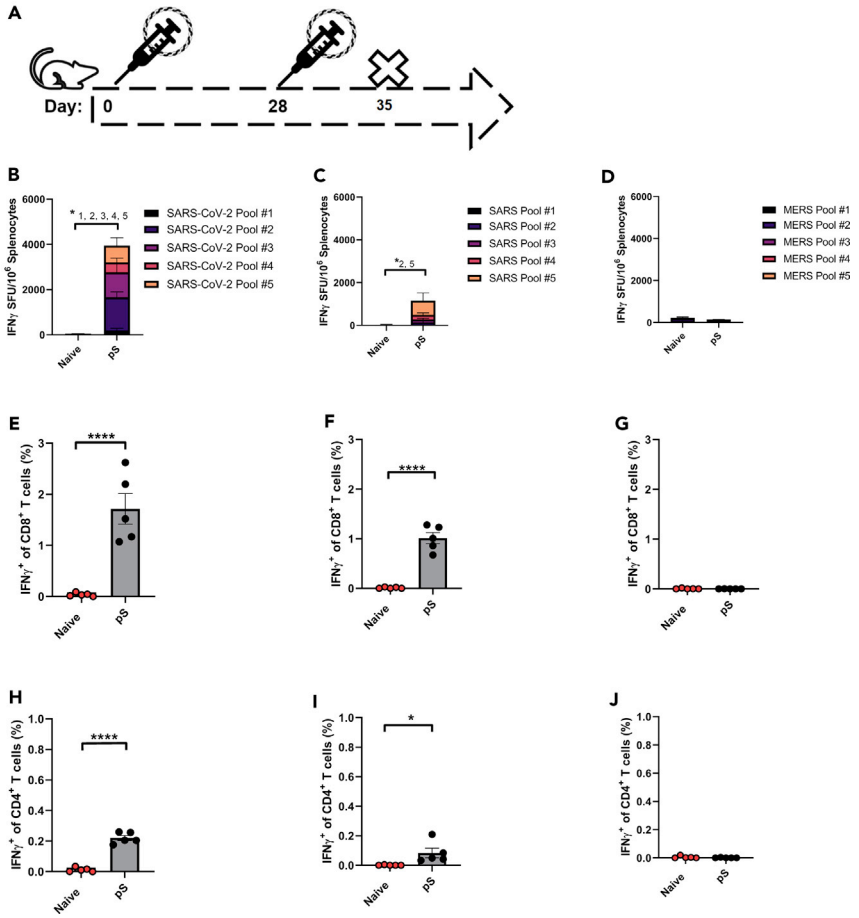

Figure 2. SARS-CoV-2 spike DNA antigens induce robust T cell immunity *in vivo*

(A) Mice were immunized twice, separated by four weeks with 10ug of plasmid DNA encoding the full-length SARS-CoV-2 spike glycoprotein (pS) or left naive, and sacrificed at day seven post-second immunization. IFNy-secreting cells were quantified in spleens by ELISpot after stimulation with overlapping peptides for SARS-CoV-2 (B), SARS-CoV-1 (C), and MERS-CoV (D) peptides. IFNy + $CD8^+$ T cells were quantified in spleens by flow cytometry after stimulation with overlapping peptides for SARS-CoV-2 (E), SARS-CoV-1 (F), and MERS-CoV (G) peptides. $IFNy^+$ $CD4^+$ T cells were quantified in spleens by flow cytometry after stimulation with overlapping peptides for SARS-CoV-2 (H), SARS-CoV-1 (I), and MERS-CoV (J) peptides. Each point represents an individual animal, bars represent the mean and error bars represent the SD. *$p < 0.05$, **$p < 0.01$, ****$p < 0.0001$ by student's t-test. Data are representative of three independent experiments with n = 5/group.

pS immunization induces robust humoral responses in mice

In order to assess the ability of pS to induce germinal center (GC) responses, we immunized mice once with 2.5ug, 10ug, or 25ug of pS and measured the frequencies of GC follicular helper T cells (T_{FH}) and B cells in local draining lymph nodes as well as serum antibodies following a single immunization. We observed a dose-dependent increase in GC T_{FH} when the dose was increased from 3.5ug to 10ug; however no significant increase was observed when increasing from 2.5ug to 25ug (Figures 3A and 3C). This was also true for the frequencies of GC B cells (Figures 3B and 3D). In keeping with this pattern, we observed significantly increased RBD-specific IgG in the serum of animals immunized with 10ug of pS but not those immunized with 25ug of pS (Figure 3E). These data indicate that the 10ug dose of pS which induces robust cellular immunity as measured by ICS and ELISpot also engenders strong GC responses including induction of T_{FH} and GC B cells. Sera from immunized animals was collected at the time of euthanasia and assayed for SARS-CoV-2 RBD specific antibody. We detected significant increases in SARS-CoV-2 RBD-specific IgG endpoint titers in the sera of immunized mice at day 7 post-second immunization (Figure 4A). Upon isotype characterization we noted increased endpoint titers of RBD-binding IgG of all isotypes (Figures 4B–4D), of

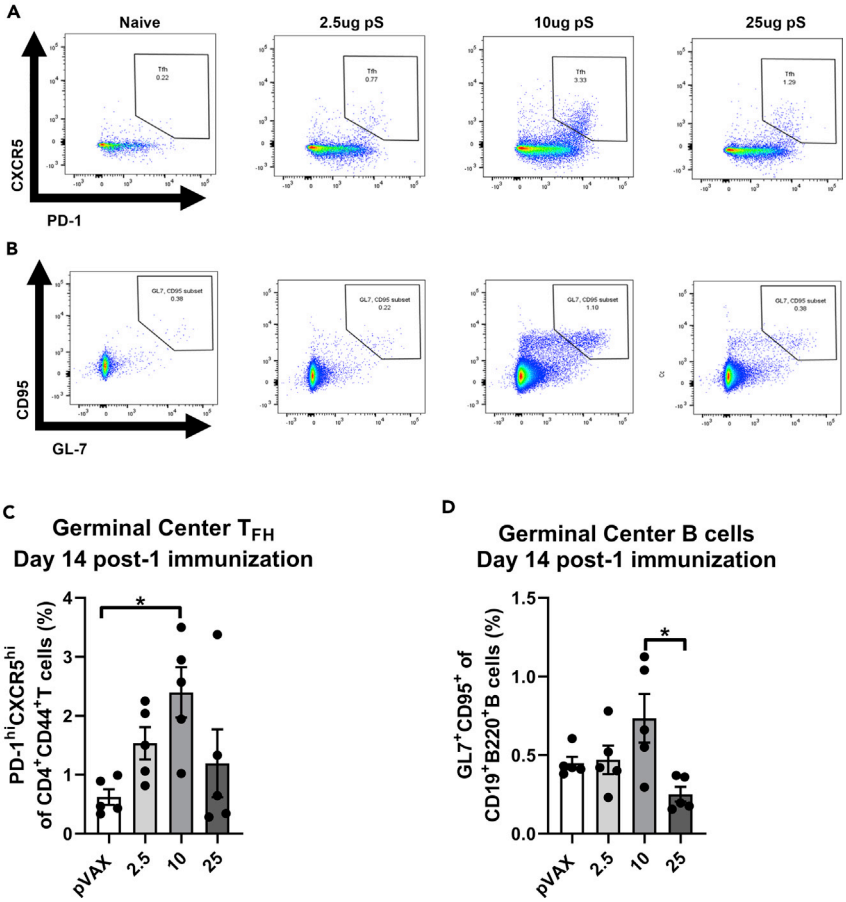

Figure 3. SARS-CoV-2 spike DNA vaccine induces germinal center formation in mice

Mice were immunized once with 2.5ug, 10ug, or 25ug of spike DNA and sacrificed at day 14 post-immunization. Popliteal and inguinal nodes from the vaccinated legs of each animal were homogenized and stained for germinal center follicular helper T cells (T_{FH}) and B cells using flow cytometry. Representative flow plots for T_{FH} (A) and GC B cells (B) and frequencies of T_{FH} (C) and GC B cells (D). Each point represents the average of duplicate assays for individual animal, bars represent the mean and error bars represent the SEM. *$p < 0.05$ by Tukey's multiple comparison test (ANOVA). Data are representative of one experiments with n = 5/group.

which IgG2a was the most prominent, with a greater than 50-fold increase in the ratio of IgG2a to IgG1 (Figure 4E), suggestive of strongly T_H1-biased immunity. In these experiments, anti-RBD antibody titers remained increased in the serum of pS immunized mice for greater than 80 days post final immunization (Figure 4F). These data suggest the pS induces robust humoral responses in mice.

In order to interrogate the functional impact of these DNA vaccine-induced SARS-CoV-2 binding antibodies, we performed *in vitro* pseudovirus neutralization assays in which SARS-CoV-2 spike pseudotyped lentiviruses were preincubated with sera from immunized animals prior to infection of huACE2-expressing CHO cells. Sera from pS-immunized mice was capable of potently inhibiting pseudoviral infectivity (Figure 4G) and displayed reciprocal ID_{50} titers that were statistically significantly increased compared to naive mouse sera (Figure 4H). Taken together these data strongly indicate that pS DNA antigens are immunogenic *in vivo*, resulting in robust anti-spike humoral immunity, which is T_H1 biased, persistent, and capable of neutralizing SARS-CoV-2 pseudoviruses *in vitro*.

pS immunization protects against SARS-CoV-2 challenge in a humanized ACE2 mouse model

Mice were immunized twice separated by four weeks with pS and rested three weeks before serum collection and delivery of AAV6.2FF-hACE2 to the entire respiratory tract using a modified intranasal

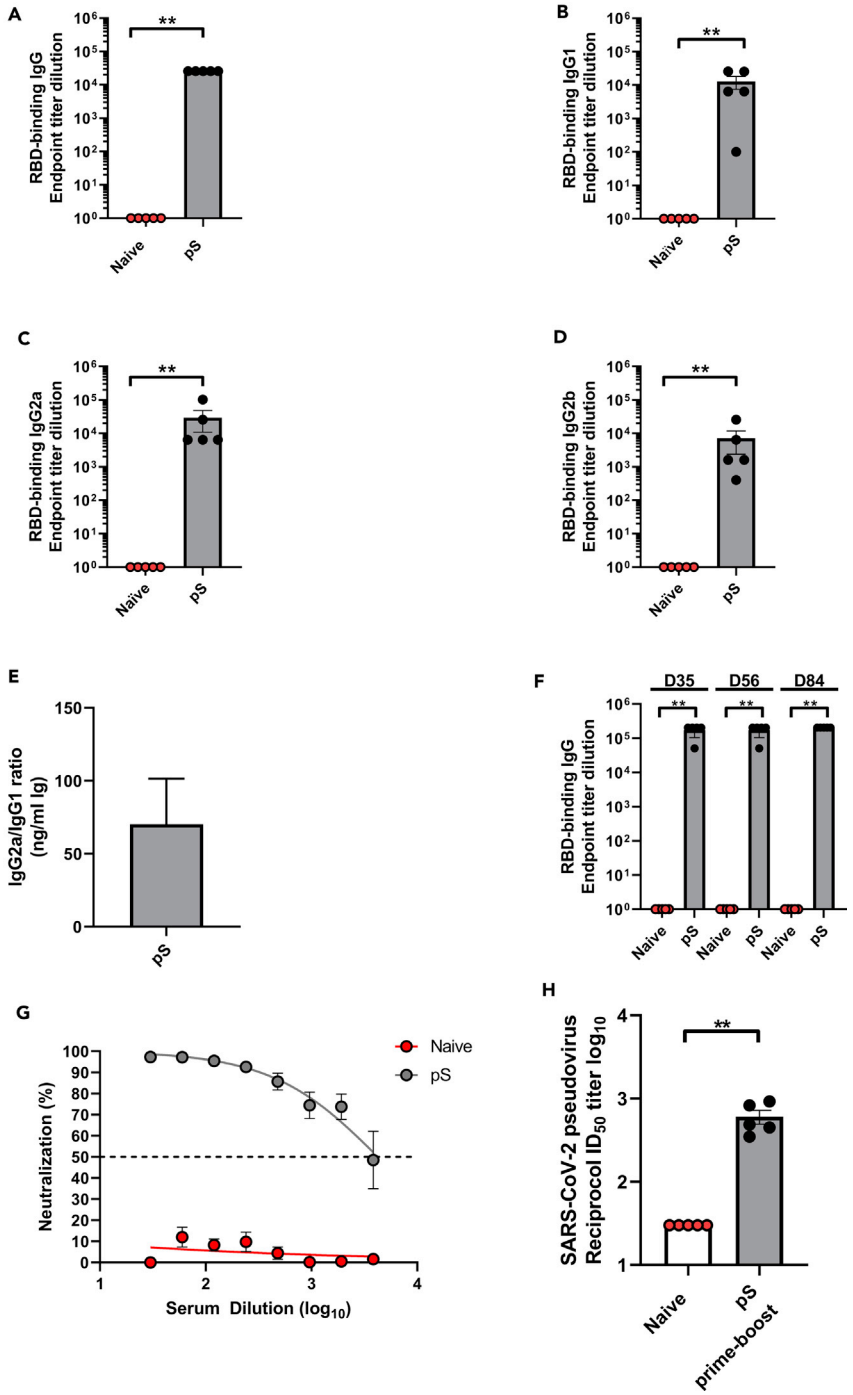

Figure 4. SARS-CoV-2 spike DNA antigens induce robust humoral immunity *in vivo*

Mice were immunized as in Figure 1 and serum was collected at day 18 post-second immunization for challenged animals and longitudinally for a second cohort of animals. Receptor binding domain (RBD)-specific IgG (A), IgG1 (B), IgG2a (C), and IgG2b (D) endpoint titers, were quantified in serum at day 7 post-second immunization and the ratio of IgG2a to IgG1 was calculated based on quantified antibody amounts (E). In a second cohort of animals, total RBD-specific IgG endpoint titers were measured longitudinally (F). SARS-CoV-2 pseudoviral neutralization percentages (G) and ID50 titers (H)were determined in serum at day 7 post-second immunization. Each point represents the average of duplicate assays for individual animal, bars represent the mean and error bars represent the SD. *p < 0.05, **p < 0.01, ****p < 0.0001 by student's t-test. Data are representative of three independent experiments with n = 5/group (A-E, G,H). Data in F are representative of one experiment.

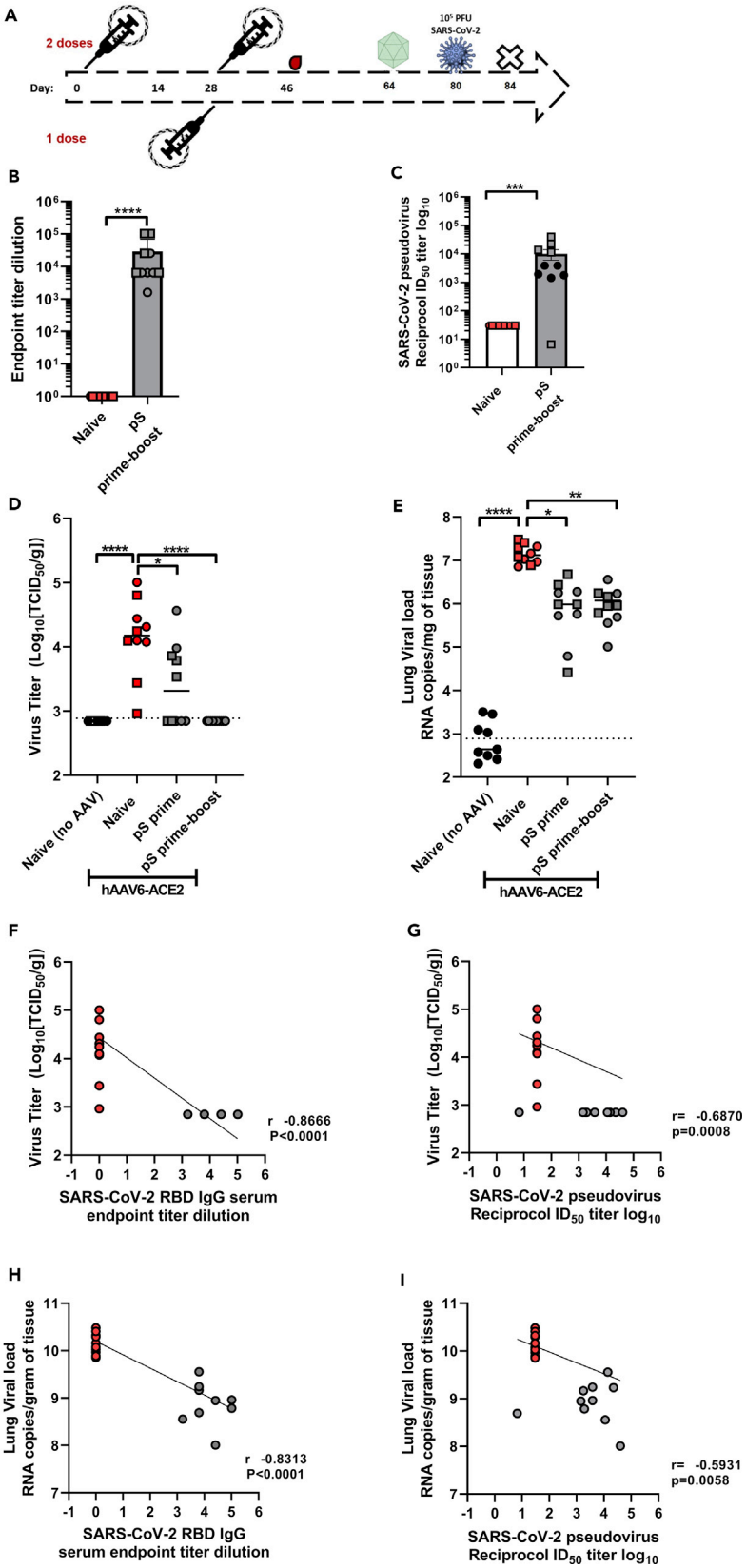
A
2 doses
1 dose
Day:
0
14
28
46
64
80
84
10⁵ PFU
SARS-CoV-2
B
Endpoint titer dilution
Naive
pS prime-boost
C
SARS-CoV-2 pseudovirus Reciprocol ID50 titer log10
Naive
pS prime-boost
D
Virus Titer (Log10[TCID50/g])
Naive (no AAV)
Naive
pS prime
pS prime-boost
hAAV6-ACE2
E
Lung Viral load RNA copies/mg of tissue
Naive (no AAV)
Naive
pS prime
pS prime-boost
hAAV6-ACE2
F
Virus Titer (Log10[TCID50/g])
r -0.8666
P<0.0001
SARS-CoV-2 RBD IgG serum endpoint titer dilution
G
Virus Titer (Log10[TCID50/g])
r= -0.6870
p=0.0008
SARS-CoV-2 pseudovirus Reciprocol ID50 titer log10
H
Lung Viral load RNA copies/gram of tissue
r -0.8313
P<0.0001
SARS-CoV-2 RBD IgG serum endpoint titer dilution
I
Lung Viral load RNA copies/gram of tissue
r= -0.5931
p=0.0058
SARS-CoV-2 pseudovirus Reciprocol ID50 titer log10

Figure 5. SARS-CoV-2 spike DNA antigens protect from viral replication *in vivo*

(A) Mice were immunized once or twice separated by four weeks with 10ug of pS via electroporation. Serum was collected at day 18 post-final immunization. At 35 days post-final immunization mice were infected intranasally with adeno-associated virus expressing human ACE2 (white). 17 days following AAV6-ACE2 transduction, animals were intranasally infected with 1×10^5 PFU of SARS-CoV-2 VIDO-01 P2. Four days post infection, animals were sacrificed to quantify viral replication. SARS-CoV-2 specific serum IgG endpoint titers (B) and pseudoviral neutralization titers (C) at day 18 post-final immunization. Replication competent virus (D), and viral RNA (E) in the lungs four-days post-infection. Pearson correlations between virus titer and serum IgG endpoints (F) and neutralization titers (G). Pearson correlations between viral RNA copies and serum IgG endpoints (H) and neutralization titers (I). Each point represents the average of duplicate samples from an individual animal, bars represent the mean, lines represent the median, and error bars represent the SD. *p < 0.05, **p < 0.01, ****p < 0.0001 by student's t-test (A and B), or Kruskall-Wallis ANOVA (D and E). Spearman correlations were used to determine relationships (F-I). Data are representative of one experiment with n = 5 males (squares) and 5 females (circles) per group.

administration method (Santry et al., 2017). Animals were rested for two weeks to allow for hACE2 expression in the lungs and then challenged with SARS-CoV-2 (VIDO-01 P2) (Figure 5A). At 3 weeks postfinal immunization, mice receiving pS had robust anti-RBD IgG end point tiers in their serum as expected (Figure 5B). Sera from pS-immunized mice remained capable of potently inhibiting SARS-CoV-2 pseudotyped virus infectivity *in vitro* (Figure 5C). Four days post-infection, mice were euthanized, and SARS-CoV-2 viral RNA and live viral titers were measured in the lung via RT-qPCR and TCID50 assay. Animals who received two doses of pS had significantly decreased SARS-CoV-2 lung viral titers (Figure 5D) and RNA (Figure 5E) in their lungs. Strikingly, a single immunization lowered viral loads in 90% of animals, and 50% of animals which received a single immunization displayed TCID50 values at or below the lower limit of detection in their lungs at the time of euthanasia (Figure 5D). Furthermore, all immunized animals had statistically significant decreases in viral RNA in the lung at this time point (Figure 5E). We observed strong inverse correlations between serum IgG endpoint titers and lung TCID50 values and viral RNA loads (Figures 5F and 5H). A similar inverse correlation was observed between neutralization titer and TCID50 and viral RNA loads post-challenge (Figures 5G and 5I). These data support a significant role for anti-SARS-CoV-2 humoral immunity in mediating protection *in vivo*.

Previous studies on vaccines targeting SARS-CoV-1 and MERS-CoV suggest that inclusion of the nucleocapsid antigen is not protective and may promote vaccine-mediated disease enhancement in challenge models. Immune responses to the nucleocapsid of SARS-CoV-2 have not been studied in great detail. However, recent evidence suggests that functional antibody responses directed against the nucleocapsid can distinguish convalescent patients from patients who succumb to COVID-19 (Atyeo et al., 2020). We designed a DNA vaccine encoding the SARS-CoV-2 nucleocapsid protein (pN) and immunized animals once with 10ug of this antigen alone or in combination with 10ug of pS (pS + pN). Immunized animals were transduced with AAV6.2FF.hACE2 followed by challenge and viral load was measured in lungs using TCID50 assay. As expected animals immunized with pN alone were unable to neutralize spike-pseudotyped viruses whole sera from animals immunized with pS alone or co-immunized with pS and pN was equally capable of neutralizing SARS-CoV-2 spike pseudotyped viruses *in vitro* (Figure S1A). Following challenge, co-immunization with pN did not significantly change the outcome of pS-mediated protection as measured by TCID50 (Figure S1B). These data suggest that nucleoprotein-directed responses alone following a single immunization were not sufficient for protection in this model.

This data supports the further study of the AAV6.2FF-hACE2 transduction model as an easily accessible small-animal model for wild-type SARS-CoV-2 infection, which may be of value in preclinical evaluation of SARS-CoV-2 targeting vaccines, such as the DNA vaccine study evaluated here, as well as likely immune-therapeutics.

DISCUSSION

We used an AAV6.2FF-hACE2-transduction model to generate long-term expression of human ACE2 in the respiratory tract of wild-type mice, making them susceptible to SARS-CoV-2 infection. Moreover, any genetically modified strain of mice (e.g. $IFNR^{-/-}$, $TLR3^{-/-}$) can be transduced with this vector making it possible to readily investigate the role of various target molecules or cells in SARS-CoV-2 replication or vaccine-mediated protection without having to cross genetically modified mouse strains with transgenic mice expressing the hACE2 receptor. A similar Ad5-hACE2-transduced mouse model has recently been described as a model for SARS-CoV-2 infection and pathogenesis (Sun et al., 2020). It is important to

note that SARS-CoV-2 has wide cellular tropism in humans and thus infection in humans is not limited solely to the respiratory tract, making this model less-applicable for studies of non-respiratory SARS-CoV-2 infection. However, based on the findings of a recent experiment in which we investigated the tropism of AAV6.2FF-mediated expression of a reporter gene, human placental alkaline phosphatase after systemic administration (Sylvia Thomas et al., ASGCT, 2020; Tracking Number: 2020-A-1527-ASGCT), it would be possible to achieve hACE2 expression in most major organs including the heart, liver, pancreas, kidney and spleen following systemic administration of AAV6.2FF-hACE2. Therefore, combined intranasal and intraperitoneal delivery of AAV6.2FF-hACE2 should allow for studies involving non-respiratory SARS-CoV-2 infection. Nevertheless, transient models of human ACE2 expression in the mouse lung such as the model used here, can provide rapid, quantifiable insights into vaccine-mediated protection until more robust models are created.

We validated the AAV6.2FF-hACE2 transduction model using plasmid DNA immunization as previously described (Smith et al., 2020). pS immunization was immunogenic and resulted in robust humoral and cell-mediated responses. We were able to detect vaccine-induced antibodies at greater than 80 days after final immunization. Cell-mediated responses to this antigen were robust as we detected increased IFNy secretion by both ELISpot and intracellular cytokine staining. While it remains unclear what role cell-mediated immunity plays in viral control in humans, it is likely that both humoral and cell-mediated immunity may be important in controlling viral replication.

Vaccine mediated enhancement or antibody-dependent enhancement (ADE) in the context of coronavirus vaccines has been previously reported(Liu et al., 2019; Hashem et al., 2019; Tseng et al., 2012; Wang et al., 2014). Most notably with live attenuated and whole inactivated vaccines (**WIVs**) (Tseng et al., 2012; Iwata-Yoshikawa et al., 2014) and T_H2-skewed vaccine regimens. Importantly, ADE has never been observed with the DNA platform for coronavirus vaccines (Yang et al., 2004; Muthumani et al., 2015; Chi et al., 2017). Indeed, we reported on the *in vivo* efficacy of an anti-MERS-CoV DNA vaccine in nonhuman primates and observed no ADE upon challenge of immunized animals (Muthumani et al., 2015), and this construct was safe and immunogenic in human patients(Modjarrad et al., 2019). In the current studies, we observed a strong T_H1 biased antibody response with a greater than 50-fold increase in the ratio of IgG2a to IgG1 in pS immunized animals. Furthermore, immunized animals were fully protected from viral replication in our challenge model, suggesting that vaccine-mediated disease enhancement in mammals for SARS-CoV-2 DNA vaccines is unlikely. Vaccination with nucleocapsid proteins has previously been reported to enhance vaccine-induced pathology in SARS-CoV-1 vaccination and challenge models and nucleocapsid-directed responses have been associated with poor prognosis in COVID-19. We therefore immunized animals DNA encoding the nucleocapsid protein of SARS-CoV-2. Thus, in this model we observed no effect on vaccine outcome when animals were immunized with nucleocapsid DNA antigens. In conclusion, AAV6.2FF transduction of human ACE2 represents a viable approach for the preclinical evaluation of SARS-CoV-2 therapeutics and prophylactics.

Limitations of the study

The AAV6.2FF huACE2 transduction model is easily accessible and allows for SARS-CoV-2 infection of mice from varied genetic backgrounds. However, intranasal delivery restricts ACE2 expression to the respiratory mucosa and thus this model does not recapitulate the biology of SARS-CoV-2 infection outside of the respiratory tract. In these studies, we used both empty-plasmid vector (pVax) control mice as well as naive mice as controls for vaccination and infection. We have previously reported that pVax immunized animals display no background response to these antigens and in these studies responses to pVax vector expressing SARS-CoV-2 nucleocapsid were not protective (Figure S1) supporting that findings of protection by SARS-CoV-2 spike DNA antigens.

STAR★METHODS

Detailed methods are provided in the online version of this paper and include the following:

- KEY RESOURCES TABLE
- RESOURCE AVAILABILITY
  - Lead contact
  - Materials availability
  - Data and code availability

SUPPLEMENTAL INFORMATION

Supplemental information can be found online at https://doi.org/10.1016/j.isci.2021.102699.

ACKNOWLEDGMENTS

The authors would like to acknowledge the Animal Facility and the flow cytometry facility at the Wistar Institute, and the facilities at PHAC for help with aspects of these studies. This work was supported in part by NIH NCI award T32 CA09171 (ENG) and NIH NIAID award T32-AI-055400 (EMP) with additional support from CEPI/Inovio Pharmaceuticals and the Wistar Institute COVID-19 science discovery fund. Graphical abstract created in BioRender.

AUTHOR CONTRIBUTIONS

E.N.G., X.Z., E.M.P., A.P., K.M., T.S., S.K.W., D.B.W., and D.K. designed experiments. E.N.G., X.Z., E.M.P., and N.J.T. performed animal immunizations. E.N.G., X.Z., E.M.P., N.J.T., M.P., J.C., S.R., K.L., E.T., A.R.A., and K.Y. performed assays. B.M.W., B.D.G., N.T., M.C., R.V., and K.L.F. performed containment challenge and viral reproduction assays. AAV6 vectors were designed and supplied by the S.K.W. laboratory and produced by Y.P., S.P.T., A.D.R., M.M.G., and S.K.W. The manuscript was written by E.N.G., B.M.W., E.M.P., B.D.G., X.Z., and N.J.T., with intellectual oversight from A.P., D.B.W., S.K.W., and D.K. The manuscript was submitted on behalf of all authors by E.N.G. and D.B.W.

DECLARATION OF INTERESTS

D.B.W. has received grant funding, participates in industry collaborations, has received speaking honoraria, and has received fees for consulting, including serving on scientific review committees and board series. Remuneration received by D.B.W. includes direct payments, stock or stock options, and in the interest of disclosure **D.B.W**. discloses the following paid associations with commercial partners: GeneOne (Consultant), Geneos (Advisory Board), Astrazeneca (Advisory Board, Speaker), Inovio (BOD, SRA, Stock), Sanofi (Advisory Board), BBI (Advisory Board).

Received: January 6, 2021
Revised: April 7, 2021
Accepted: June 7, 2021
Published: July 23, 2021

REFERENCES

Atyeo, C., Fischinger, S., Zohar, T., Slein, M.D., Burke, J., Loos, C., Mcculloch, D.J., Newman, K.L., Wolf, C., and Yu, J.J.I. (2020). Distinct Early Serological Signatures Track with SARS-CoV-2 Survival. Immunity *53*, 524–532.e4.

Aurnhammer, C., Haase, M., Muether, N., Hausl, M., Rauschhuber, C., Huber, I., Nitschko, H., Busch, U., Sing, A., Ehrhardt, A., and Baiker, A. (2012). Universal real-time PCR for the detection and quantification of adeno-associated virus serotype 2-derived inverted terminal repeat sequences. Hum. Gene Ther. Methods *23*, 18–28.

Balazs, A.B., Chen, J., Hong, C.M., Rao, D.S., Yang, L., and Baltimore, D. (2012). Antibody-based protection against HIV infection by vectored immunoprophylaxis. Nature *481*, 81–84.

Bao, L., Deng, W., Huang, B., Gao, H., Liu, J., Ren, L., Wei, Q., Yu, P., Xu, Y., Qi, F., et al. (2020). The pathogenicity of SARS-CoV-2 in hACE2 transgenic mice. Nature *583*, 830–833.

Chi, H., Zheng, X., Wang, X., Wang, C., Wang, H., Gai, W., Perlman, S., Yang, S., Zhao, J., and Xia, X.J.V. (2017). DNA vaccine encoding Middle East respiratory syndrome coronavirus S1 protein induces protective immune responses in mice *35*, 2069–2075.

Hashem, A.M., Algaissi, A., Agrawal, A., Al-Amri, S., Almasoud, A., Alharbi, N., Peng, B.-H., Li, X., and Tseng, C.-T. (2019). CD40-targeted S1 subunit vaccine protects against MERS-CoV and S1-associated pulmonary immunopathology in transgenic human DPP4 mouse model. J. Immunol. *202*, 139.10.

Hassan, A.O., Case, J.B., Winkler, E.S., Thackray, L.B., Kafai, N.M., Bailey, A.L., Mccune, B.T., Fox, J.M., Chen, R.E., and Alsoussi, W.B.J.C. (2020). A

SARS-CoV-2 infection model in mice demonstrates protection by neutralizing antibodies *182*, 744–753.e4.

Huang, C., Wang, Y., Li, X., Ren, L., Zhao, J., Hu, Y., Zhang, L., Fan, G., Xu, J., and Gu, X. (2020). Clinical features of patients infected with 2019 novel coronavirus in Wuhan, China. Lancet *395*, 497–506.

Imai, M., Iwatsuki-Horimoto, K., Hatta, M., Loeber, S., Halfmann, P.J., Nakajima, N., Watanabe, T., Ujie, M., Takahashi, K., and Ito, M. (2020). Syrian hamsters as a small animal model for SARS-CoV-2 infection and countermeasure development. Proc. Natl. Acad. Sci. U S A *117*, 16587–16595.

Iwata-Yoshikawa, N., Uda, A., Suzuki, T., Tsunetsugu-Yokota, Y., Sato, Y., Morikawa, S., Tashiro, M., Sata, T., Hasegawa, H., and Nagata, N.J.J.O.V. (2014). Effects of Toll-like receptor stimulation on eosinophilic infiltration in lungs of BALB/c mice immunized with UV-inactivated severe acute respiratory syndrome-related coronavirus vaccine. J. Virol. *88*, 8597–8614.

Jin, X., Lian, J.-S., Hu, J.-H., Gao, J., Zheng, L., Zhang, Y.-M., Hao, S.-R., Jia, H.-Y., Cai, H., and Zhang, X.-L. (2020). Epidemiological, clinical and virological characteristics of 74 cases of coronavirus-infected disease 2019 (COVID-19) with gastrointestinal symptoms. Gut *69*, 1002–1009.

Kang, M.H., van Lieshout, L.P., Xu, L., Domm, J.M., Vadivel, A., Renesme, L., Mühlfeld, C., Hurskainen, M., Mižíková, I., Pei, Y., et al. (2020). A lung tropic AAV vector improves survival in a mouse model of surfactant B deficiency. Nat. Commun. *11*, 3929.

Liu, L., Wei, Q., Lin, Q., Fang, J., Wang, H., Kwok, H., Tang, H., Nishiura, K., Peng, J., and Tan, Z. (2019). Anti–spike IgG causes severe acute lung injury by skewing macrophage responses during acute SARS-CoV infection. JCI Insight *4*, e123158.

Modjarrad, K., Roberts, C.C., Mills, K.T., Castellano, A.R., Paolino, K., Muthumani, K., Reuschel, E.L., Robb, M.L., Racine, T., and Oh, M.-D. (2019). Safety and immunogenicity of an anti-Middle East respiratory syndrome coronavirus DNA vaccine: a phase 1, open-label, single-arm, dose-escalation trial *19*, 1013–1022.

Moreau, G.B., Burgess, S.L., Sturek, J.M., Donlan, A.N., Petri, W.A., JR., and Mann, B.J. (2020). Evaluation of K18-hACE2 mice as a model of SARS-CoV-2 infection. Am. J. Trop. Med. Hyg. *103*, 1215–1219.

Muthumani, K., Falzarano, D., Reuschel, E.L., Tingey, C., Flingai, S., Villarreal, D.O., Wise, M., Patel, A., Izmirly, A., and Aljuaid, A. (2015). A synthetic consensus anti–spike protein DNA vaccine induces protective immunity against Middle East respiratory syndrome coronavirus in nonhuman primates. Sci. Transl Med. *7*, 301ra132.

Santry, L.A., Ingrao, J.C., Darrick, L.Y., de Jong, J.G., van Lieshout, L.P., Wood, G.A., and Wootton, S.K. (2017). AAV vector distribution in the mouse respiratory tract following four different methods of administration. BMC Biotechnol. *17*, 43.

Smith, T.R., Patel, A., Ramos, S., Elwood, D., Zhu, X., Yan, J., Gary, E.N., Walker, S.N., Schultheis, K., and Purwar, M. (2020). Immunogenicity of a DNA vaccine candidate for COVID-19. Nat. Commun. *11*, 1–13.

Sun, J., Zhuang, Z., Zheng, J., LI, K., Wong, R.L.-Y., Liu, D., Huang, J., He, J., Zhu, A., and Zhao, J. (2020). Generation of a broadly useful model for COVID-19 pathogenesis, vaccination, and treatment. Cell *182*, 734–743.e5.

Tseng, C.-T., Sbrana, E., Iwata-Yoshikawa, N., Newman, P.C., Garron, T., Atmar, R.L., Peters, C.J., and Couch, R.B. (2012). Immunization with SARS coronavirus vaccines leads to pulmonary immunopathology on challenge with the SARS virus. PLoS One *7*, e35421.

van Lieshout, L.P., Domm, J.M., Rindler, T.N., Frost, K.L., Sorensen, D.L., Medina, S.J., Booth, S.A., Bridges, J.P., and Wootton, S.K. (2018). A novel triple-mutant AAV6 capsid induces rapid and potent transgene expression in the muscle and respiratory tract of mice. Mol. Ther. Methods Clin. Dev. *9*, 323–329.

van Lieshout, L.P., Domm, J.M., and Wootton, S.K. (2019). AAV-mediated gene delivery to the lung. Methods Mol. Biol. *1950*, 361–372.

Wang, S.-F., Tseng, S.-P., Yen, C.-H., Yang, J.-Y., Tsao, C.-H., Shen, C.-W., Chen, K.-H., Liu, F.-T., LIU, W.-T., and Chen, Y.-M. (2014). Antibody-dependent SARS coronavirus infection is mediated by antibodies against spike proteins. Biochem Biophys Res Commun. *451*, 208–214.

Winkler, E.S., Bailey, A.L., Kafai, N.M., Nair, S., Mccune, B.T., Yu, J., Fox, J.M., Chen, R.E., Earnest, J.T., and Keeler, S.P.J.N.I. (2020). SARS-CoV-2 infection of human ACE2-transgenic mice causes severe lung inflammation and impaired function. Nat. Immunol. *21*, 1327–1335.

Yang, X.-H., Deng, W., Tong, Z., Liu, Y.-X., Zhang, L.-F., Zhu, H., Gao, H., Huang, L., Liu, Y.-L., and Ma, C.-M. (2007). Mice transgenic for human angiotensin-converting enzyme 2 provide a model for SARS coronavirus infection. Comp. Med. *57*, 450–459.

Yang, Z.-Y., Kong, W.-P., Huang, Y., Roberts, A., Murphy, B.R., Subbarao, K., and Nabel, G.J. (2004). A DNA vaccine induces SARS coronavirus neutralization and protective immunity in mice. Nature *428*, 561–564.

Zhou, P., Yang, X.-L., Wang, X.-G., Hu, B., Zhang, L., Zhang, W., Si, H.-R., Zhu, Y., Li, B., and Huang, C.-L. (2020). A pneumonia outbreak associated with a new coronavirus of probable bat origin. Nature *579*, 270–273.

Zhu, N., Zhang, D., Wang, W., Li, X., Yang, B., Song, J., Zhao, X., Huang, B., Shi, W., and Lu, R. (2020). A novel coronavirus from patients with pneumonia in China, 2019. New Engl. J. Med. *382*, 727–733.

Zost, S.J., Gilchuk, P., Case, J.B., Binshtein, E., Chen, R.E., Nkolola, J.P., Schäfer, A., Reidy, J.X., Trivette, A., and Nargi, R.S. (2020). Potently neutralizing and protective human antibodies against SARS-CoV-2. Nature *584*, 443–449.

STAR★METHODS

KEY RESOURCES TABLE

REAGENT or RESOURCE	SOURCE	IDENTIFIER
Antibodies		
anti-mouse CD8	Biolegend	Cat# 100742; RRID: AB_11124344
anti-mouse CD4	Biolegend	Cat# 100447; RRID: AB_2564586
anti-mouse CD3e	Biolegend	Cat# 100216; RRID: AB_49369
anti-mouse CD107a	Biolegend	Cat# 121606; RRID: AB_572007
anti-mouse IFNγ	Biolegend	Cat# 505810; RRID: AB_315404
anti-mouse TNFα	Biolegend	Cat# 506346; RRID: AB_2565955
anti-mouse IL-2	Biolegend	Cat# 503832; RRID: AB_2561750
anti-mouse CD62L	Biolegend	Cat# 104445; RRID: AB_2564215
anti-mouse CXCR5	Biolegend	Cat# 145520; RRID: AB_2562866
anti-mouse PD-1	Biolegend	Cat# 135206; RRID: AB_1877231
anti-mouse IgG(h+l)-HRP	Bethyl	Cat# A90-216P
Bacterial and virus strains		
SARS-CoV-2; hCoV-19/Canada/ ON-VIDO-01/2020	BEI resources	GISAID: EPI_ISL_425177 BEI: NR-53565
Chemicals, peptides, and recombinant proteins		
SARS-COV-2 spike peptides	Genscript	Custom peptide llibrary created to match DNA plasmid antigens
Critical commercial assays		
Mouse IFNy ELISpot kit	Mabtech	3321-4APT-10
Experimental models: cell lines		
CHO-ACE2 cell line	Creativebiolabs	VCeL-Wyb019
Recombinant DNA		
SARS-CoV-2 spike DNA plasmid	Genscript	proprietary
SARS-CoV-2 nucleocapsid DNA plasmid	Genscript	proprietary
Software and algorithms		
Prism v. 9	Graphpad	V9.1.1(225)
Flowjo v.10	Treestar	v10.7.2

RESOURCE AVAILABILITY

Lead contact

Further information and requests for resources and reagents should be directed to lead contacts, Dr. Darwyn Kobasa at the Public Health Agency of Canada (darwyn.kobasa@canada.ca) for animal challenge model studies, Dr. David B. Weiner at the Wistar Institute (dweiner@wistar.org) for vaccination studies, Dr. Sarah Wootton at the University of Guelph (kwootton@uoguelph.canada.ca) for AAV6 vectors, and Dr. Trevor Smith at Inovio pharmaceuticals (tsmith@inovio.com) for DNA plasmids.

Materials availability

This study generated unique DNA plasmid immunogens and matched peptides as well as ACE2-expressing modified AAV6 vectors and SARS-CoV-2 pseudotyped viruses. Please contact listed lead investigators for materials availability.

Data and code availability

The published article includes all data sets generated or analyzed during this study.

EXPERIMENTAL MODELS AND SUBJECT DETAILS

Animals and immunization

6-8 week-old female C57BL/6 and BALB/c were purchased from The Jackson Laboratory and were housed in the Wistar Institute Animal Facility. 10μg of DNA plasmid encoding SARS-CoV-2 Spike glycoprotein (pS) alone, SARS-CoV-2 nucleocapsid protein (pN) alone, or 10ug of pS and 10ug of pN in 30μL water was injected in the tibialis anterior (TA) muscle, followed by delivery of two 0.1 Amp electric constant current square-wave pulses by the CELECTRA-3P electroporation device (Inovio Pharmaceuticals) to increase transfection efficiency. The vaccine schedule is indicated in each figure. All procedures were done in accordance with the guidelines from the Wistar Institute Animal Care and Use Committee. Submandibular bleeds were taken weekly to isolate sera for future assays. Blood via cardiac puncture, spleens, and Bronchoalveolar lavage (**BAL**) fluid were collected at the time of euthanasia.

Pseudovirus neutralization assay

SARS-CoV-2 pseudovirus were produced using HEK293T cells transfected with 1:1 ratio of IgE-SARS-CoV-2 S plasmid (Genscript) and pNL4-3.Luc.R-E- plasmid (NIH AIDS reagent) using Gene jammer (Agilent) as transfection reagent. Forty-eight hours post-transfection, transfection supernatant was collected, enriched with FBS to 12% final volume, and stored at -80°C. SARS-Cov-2 pseudovirus neutralization assay was set up using D10 media (DMEM supplemented with 10% FBS and 1 X Penicillin-Streptomycin) in a 96 well format using huCHOAce2 cells (Creative Biolabs, Catalog No. VCeL-Wyb019). For neutralization assay, 10,000 CHO-ACE2 cells were plated in 96-well plates and rested overnight at 37°C and 5% CO2 for 24 hours. Following day, sera from INO-4800 vaccinated and control groups were heat inactivated and serially diluted as desired. Sera were incubated with a fixed amount of SARS-Cov-2 pseudovirus for 90 minutes at RT following which the mix was added to huCHOAce2 cells and allowed to incubate in a standard incubator (37% humidity, 5% CO2) for 72h. Post 72h, cells were lysed using britelite plus luminescence reporter gene assay system (Perkin Elmer Catalog no. 6066769) and RLU were measured using the Biotek plate reader. Neutralization titers (ID50) were calculated using GraphPad Prism 8 and defined as the reciprocal serum dilution at which RLU were reduced by 50% compared to RLU in virus control wells after subtraction of background RLU in cell control wells.

Generation of AAV6.2FF-hACE2

The cDNA for human ACE2 (SinoBiological; HG10108-M) was cloned into an AAV genome plasmid (pACASI-MSC-WPRE) containing the composite CASI promoter (Balazs et al., 2012) consisting of the human cytomegalovirus immediate-early gene enhancer region, the chicken beta actin promoter, and the human ubiquitin C promoter, as well as the woodchuck hepatitis virus posttranscriptional regulatory element (WPRE) and simian virus 40 polyadenylation sequence downstream of hACE2 with flanking AAV2 inverted terminal repeats (ITRs). The hACE2 gene was amplified with Inf-AAV-ACE2-KpnI-F (5′-GGGTGACGAA CAGGGTACCGCCACCATGTCAAGCTCTTCCTGGCTC-3′) and Inf-AAV-ACE2-XbaI-R (5′-CAGAGGT TGATTATTCTAGACTAAAAGGAGGTCTGAACATC-3′) primers and cloned into the KpnI-XbaI site of pACASI-MSC-WPRE using In-Fusion Cloning (Takara Bio) as per the manufacturer's instructions. An AAV vector expressing firefly luciferase (AAV-Luc) from the same AAV genome was described previously (Kang et al., 2020). AAV6.2FF pseudotyped vectors were produced by co-transfection of human embryonic kidney 293 cells with genome and packaging plasmids and purified with heparin columns as described previously (van Lieshout et al., 2019). AAV vector titers were determined by quantitative polymerase chain reaction (qPCR) analysis as described elsewhere (Aurnhammer et al., 2012).

SARS-CoV-2 challenge

For challenge with SARS-CoV-2, all mice were anaesthetized with inhalation isoflurane. Mice were administered 10^{11} viral genomes of either AAV6.2FF-Luc or AAV6.2FF-hACE2 intranasally in 50μL (25μL per nare). For SARS-CoV-2 infection, on either day 11 (initial characterization) or day 14 (vaccine efficacy experiments) post-AAV infection, virus (SARS-CoV-2; hCoV-19/Canada/ON-VIDO-01/2020, GISAID accession# EPI_ISL_425177) was diluted in plain media and animals were administered 10^5 $TCID_{50}$ intranasally in 50μL (25μL per nare). Animals were recovered and then weighed and monitored daily for any clinical signs of disease. On days 2 and 4 post-infection for model development and day 4 post-infection for vaccine studies,

animals were euthanized to examine viral replication in the respiratory tract. Euthanasia was performed by cervical dislocation following anesthesia with inhaled isoflurane.

METHOD DETAILS

ELISpot assay

Spleens from immunized mice were harvested and stored in RPMI 1640 media (Invitrogen) before being dissociated by a stomacher. Red blood cells were removed by ACK lysing buffer. The splenocytes were filtered and counted. 2 x 10^5 splenocytes were plated into each well on Mouse IFN-γ ELISpot^{PLUS} plates (Mabtech) and stimulated for 20 hours with SARS-CoV-1, SARS-CoV-2, or MERS-CoV peptides (15-mer peptides overlapping by 9 amino acid from the native SARS-CoV-1, SARS-CoV-2, or MERS-CoV proteins, Genscript). Cells were stimulated with 5μg/mL of each peptide in complete media (R10). The spots were developed based on manufacturer's instructions. R10 and cell stimulation cocktails (Invitrogen) were used for negative and positive controls, respectively. Spots were scanned and quantified by ImmunoSpot CTL reader. Spot-forming unit (SFU) per million cells was calculated by subtracting the negative control wells.

Intracellular cytokine staining and flow cytometry

Wells were seeded with 1,000,000 cells in 100 μL of R10. Cells were stimulated with peptides from SARS-CoV-2, SARS-CoV, or MERS-CoV proteins *at a final concentration of 5 μg/mL per peptide in the presence of Protein Transport Inhibitor (eBioscience, San Diego, CA, USA). R10 and Cell Stimulation Cocktail (eBioscience, San Diego, CA, USA) were used as negative and positive controls, respectively. Plates were incubated for 5 h at 37°C with 5% CO_2.*Splenocytes were stimulated by peptides for 5 hours with protein transport inhibitor (Invitrogen). After stimulation, cells were stained with LIVE/DEAD violet for viability. CD3e (17A2), CD4 (RM4-5), CD8b (YTS156.7.7), IFN-γ (XMG1.2), TNF-α(MP6-XT22), and IL-2 (JES56-5H4) fluorochrome conjugated antibodies (all from BioLegend) were used for surface and intracellular staining. The samples were run on an 18-color LSRII flow cytometer (BD Biosciences) and analyzed by FlowJo software. Gates were set using FMOs for each stain. Data were exported and analyzed in GraphPad Prism 8.1.1.

ELISA

For binding and quantification of serum and BAL antibodies, NUNC MaxiSorp 96-well plates (Thermo Scientific) were coated with 1μg/mL RBD of SARS-CoV-2 spike protein (Genscript) in PBS overnight at 4°C. The following day, plates were washed with PBS-0.5% Tween 20 and blocked with PBS-10% fetal bovine serum. Next, the plates were again washed and subsequently incubated with diluted mouse sera for two hours. Following primary serum incubation, plates were incubated with goat anti-mouse IgG-HRP (Bethyl) for one hour at room temperature. TMB (Thermo) was used to develop the binding signal. Upon stopping with 1N sulfuric acid, plates were read with the BioTek Synergy 2 plate reader (BioTek) at 450nm. Data were subsequently exported to Microsoft Excel and analyzed in graphpad prism version 8.

QUANTIFICATION AND STATISTICAL ANALYSIS

Statistical analysis

All statistics were analyzed using GraphPad Prism 8. Error bars represent means ± SEM or the mean ± SD where denoted. Normality was determined using the Shapiro-Wilk normality test. Outliers were determined and removed using the ROUT algorithm. For data deemed normal, ordinary one-way analysis of variance (ANOVA) was performed to determine statistical significance between groups of three or more (Tukey's multiple comparison test). For data deemed non-normal, a non-parametric Kruskal-Wallis test was performed in order to determine statistical differences between groups of three or more. Statistical differences between groups of two were determined via unpaired t test for data deemed normal, or Mann-Whitney U test for data deemed non-normal. In all data *p<0.05, **p<0.01, ***p<0.001, and ****p<0.0001.